Article

Determination of Peptide Oligomerization in Lipid Bilayers Using ^{19}F Spin Diffusion NMR

Jarrod J. Buffy, Alan J. Waring, and Mei Hong

J. Am. Chem. Soc., **2005**, 127 (12), 4477-4483• DOI: 10.1021/ja043621r • Publication Date (Web): 26 February 2005

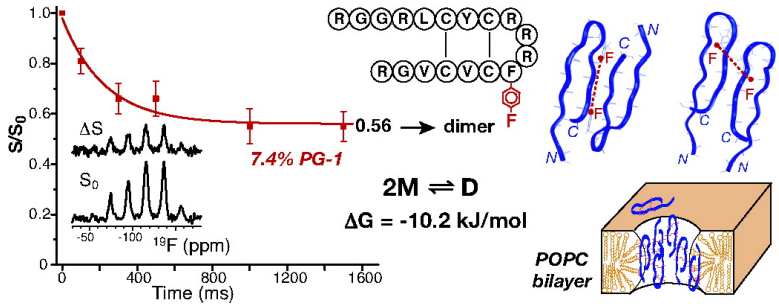

More About This Article

Additional resources and features associated with this article are available within the HTML version:

- Supporting Information
- Links to the 8 articles that cite this article, as of the time of this article download
- Access to high resolution figures
- Links to articles and content related to this article
- Copyright permission to reproduce figures and/or text from this article

View the Full Text HTML

J|A|C|S
ARTICLES
Published on Web 02/26/2005

Determination of Peptide Oligomerization in Lipid Bilayers Using ^{19}F Spin Diffusion NMR

Jarrod J. Buffy,[†,‡] Alan J. Waring,[§] and Mei Hong*[,†]

Contribution from the Department of Chemistry, Iowa State University, Ames, Iowa 50011, and Department of Medicine, University of California at Los Angeles School of Medicine, Los Angeles, California 90095

Received October 20, 2004; E-mail: mhong@iastate.edu

Abstract: Aggregation or oligomerization is important for the function of many membrane peptides such as ion channels and antimicrobial peptides. However, direct proof of aggregation and the determination of the number of molecules in the aggregate have been difficult due to the lack of suitable high-resolution methods for membrane peptides. We propose a ^{19}F spin diffusion magic-angle-spinning NMR technique to determine the oligomeric state of peptides bound to the lipid bilayer. Magnetization transfer between chemically equivalent but orientationally different ^{19}F spins on different molecules reduces the ^{19}F magnetization in an exchange experiment. At long mixing times, the equilibrium ^{19}F magnetization is $1/M$, where M is the number of orientationally different molecules in the aggregate. The use of the ^{19}F spin increases the homonuclear dipolar coupling and thus the distance reach. We demonstrate this technique on crystalline model compounds with known numbers of molecules in the asymmetric unit cell, and show that ^{19}F spin diffusion is more efficient than that of ^{13}C by a factor of $\sim$500. Application to a β-hairpin antimicrobial peptide, protegrin-1, shows that the peptide is almost completely dimerized in POPC bilayers at a concentration of 7.4 mol %. Decreasing the peptide concentration reduced the dimer fraction. Using a monomer−dimer equilibrium model, we estimate the ΔG for dimer formation to be -10.2 ± 2.3 kJ/mol. This is in good agreement with the previously measured free energy reduction for partitioning and aggregating β-sheet peptides into phospholipid membranes. This ^{19}F spin diffusion technique opens the possibility of determining the oligomeric structures of membrane peptides.

Introduction

The intermolecular association or aggregation of peptides and proteins is ubiquitous in nature, and can have beneficial or deleterious consequences. Amyloids, insoluble fibril-forming protein aggregates, are implicated in neurodegenerative diseases such as Alzheimer's, Huntington's, and bovine spongiform encephalopathy.[1] A growing number of solid-state NMR investigations have been reported on the supramolecular assembly of amyloidogenic peptides.[2,3] In biological membranes, many peptides and proteins require oligomerization of multiple subunits or self-association for function.[4] Two well-studied cases of functionally important homooligomerization are the helical peptides glycophorin A and the transmembrane domain of the M2 protein of influenza A.[5−7] Despite the prevalence of membrane peptide oligomerization and the importance of understanding the thermodynamics of aggregation, no high-resolution methods are so far available to directly determine the oligomeric state of membrane peptides, let alone the detailed aggregate structure, due to the general difficulty of investigating peptide structure in lipid bilayers. Instead, analytical ultracentrifugation, equilibrium dialysis, and other biochemical approaches have been employed to probe the folding and self-association of membrane peptides.[6−9]

Solid-state NMR is becoming an increasingly important spectroscopic technique to study the three-dimensional structures of membrane peptides and proteins directly in the biologically relevant environment of the lipid bilayer. The orientation of membrane peptides relative to the bilayer normal,[10] the high-resolution structure of protein−ligand interfaces,[11] and peptide−lipid interactions[12,13] can be determined with exquisite detail

[†] Iowa State University.
[‡] Current address: Department of Chemistry, University of Minnesota, Minneapolis, MN 55455.
[§] University of California at Los Angeles School of Medicine.

(1) Murphy, R. M. *Annu. Rev. Biomed. Eng.* **2002**, *4*, 155−174.
(2) Petkova, A. T.; Ishii, Y.; Balbach, J. J.; Antzutkin, O. N.; Leapman, R. D.; Delaglio, F.; Tycko, R. *Proc. Natl. Acad. Sci. U.S.A.* **2002**, *99*, 16742−16747.
(3) Jaroniec, C. P.; MacPhee, C. E.; Bajaj, V. S.; McMahon, M. T.; Dobson, C. M.; Griffin, R. G. *Proc. Natl. Acad. Sci. U.S.A.* **2004**, *101*, 711−716.
(4) Lehninger, A. L.; Nelson, D. L.; Cox, M. M. *Principles of Biochemistry*, 2nd ed.; Worth Publishers: New York, 1993.
(5) DeGrado, W. F.; Gratkowski, H.; Lear, J. D. *Protein Sci.* **2003**, *12*, 647−665.
(6) Howard, K. P.; Lear, J. D.; DeGrado, W. F. *Proc. Natl. Acad. Sci. U.S.A.* **2002**, *99*, 8568−8572.
(7) MacKenzie, K. R.; Prestegard, J. H.; Engelman, D. M. *Science* **1997**, *276*, 131−133.
(8) Wimley, W. C.; Hristova, K.; Ladokhin, A. S.; Silverstro, L.; Axelsen, P. H.; White, S. H. *J. Mol. Biol.* **1998**, *277*, 1091−1110.
(9) Cristian, L.; Lear, J. D.; DeGrado, W. F. *Proc. Natl. Acad. Sci. U.S.A.* **2003**, *100*, 14772−14777.
(10) Opella, S. J.; Nevzorov, A.; Mesleb MF, M. F. *Biochem. Cell Biol.* **2002**, *80*, 597−604.
(11) McDermott, A. E.; Creuzet, F.; Gebhard, R.; Hoef, K. v. d.; Levitt, M. H.; Herzfeld, J.; Herzfeld, J.; Lugtenburg, J.; Griffin, R. G. *Biochemistry* **1994**, *33*, 6129−6136.
(12) Auger, M. *Curr. Issues Mol. Biol.* **2000**, *2*, 119−124.

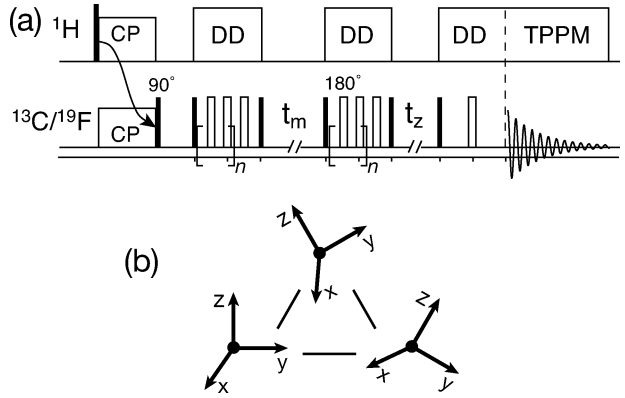

Figure 1. (a) Pulse sequence for the CODEX experiment. Filled and open rectangles indicate 90° and 180° pulses, respectively. DD = dipolar decoupling. TPPM = two-pulse phase modulation[57] to enhance the X nucleus spectral resolution. (b) Principle of CODEX for determining the number of molecules in an aggregate on the basis of orientational inequivalence. A molecule-fixed chemical shift tensor experiences M different orientations in the aggregate. After complete exchange, the remaining magnetization on the initial molecule is $1/M$. This is detected in the CODEX experiment as the S/S_0 value at equilibrium.

using solid-state NMR. However, the traditional arsenal of solid-state NMR has not allowed for the determination of the size of membrane peptide oligomers. The most promising approach is multiple-quantum (MQ) NMR: excitation of MQ coherences among homonuclear dipolar-coupled spins allows intermolecular spin counting within a distance determined by the strength of the dipolar coupling. Unfortunately, MQ NMR is most suitable for static samples; thus, it suffers from inherently low sensitivity.[14,15]

Here we propose and demonstrate a ^{19}F spin diffusion technique, applicable under the magic-angle-spinning (MAS) condition to ensure high sensitivity, for determining the aggregation number of membrane peptides. We detect spin diffusion using the CODEX (centerband-only detection of exchange) pulse sequence,[16,17] which was originally designed to probe slow molecular reorientations on the time scale of 1 ms or longer. The technique utilizes the recoupled chemical shift anisotropy (CSA) to sample the orientational change of molecules due to slow motion or spin diffusion between sites with different chemical shift tensor orientations.[17] The CSA recoupling, achieved by rotor-synchronized 180° (π) pulses, occurs in two stages that are separated by a mixing period, $90°-\tau_m-90°$, without ^{1}H decoupling, during which motion and spin diffusion can occur (Figure 1a). In the absence of orientational changes, the CSA evolution is completely refocused by the end of the second π-pulse train, giving rise to a stimulated echo. Reorientation during τ_m due to motion or spin diffusion changes the anisotropic frequency, thus decreasing the echo intensity. When slow motion is eliminated through sample cooling, the CODEX experiment detects only spin diffusion. This spin diffusion is mediated by the dipolar coupling between the X spins and facilitated by the coupling of the X spins to the ^{1}H spin reservoir.[18,19] For spin diffusion between two X spins with identical isotropic chemical shifts but different anisotropic shifts, the case of relevance here, the rate of spin diffusion is proportional to $K_{ij}^2 f_{ij}(0)$. Here K_{ij}^2 depends on both the dipolar coupling and the incidental chemical shift tensor difference between the two X spins,[20] and $f_{ij}(0)$ is the overlap integral between the single-quantum signals of the two X spins. With zero isotropic shift difference, the CSA- and dipolar-driven spin diffusion may also be considered as $n = 0$ rotational resonance with strong zero-quantum dephasing due to the couplings to protons.[20] This leads to an exponential decay of the difference magnetization with the mixing time. For homogeneous systems consisting of a single oligomeric species with M orientationally unique molecules, the equilibrium S/S_0 value at long mixing times is $1/M$, since only $1/M$ of the magnetization resides in the original molecule (Figure 1b). Thus, by measuring the equilibrium value of a spin diffusion CODEX experiment, one can extract the size of a peptide aggregate.

While ^{13}C CODEX has been used to a limited extent in model compounds for measuring spin diffusion coefficients,[21] the weak $^{13}C-^{13}C$ dipolar couplings limit the maximum detectable distance, making ^{13}C CODEX undesirable for studying membrane peptide aggregation. The high gyromagnetic ratio (γ) and large chemical shift anisotropy of ^{19}F spins, on the other hand, are extremely useful for probing long distances and molecular orientations. ^{19}F dipolar recoupling under MAS has been shown to yield intramolecular distances up to 12 Å in small organic compounds with several different fluorine sites.[22] Fluorinated amino acids such as [^{19}F]-4-fluorophenylglycine have been incorporated into membrane peptides to determine peptide orientations with respect to the bilayer normal.[23−25] Long-range distances between ^{19}F and other spin-1/2 nuclei such as ^{31}P and ^{1}H have also been measured in a number of complex systems such as enzyme−substrate complexes.[26−28]

In this work, we demonstrate the combined use of the $1/M$ equilibrium principle of spin diffusion CODEX with ^{19}F detection to determine the mode of oligomerization of membrane peptides. We first show the long-distance reach of ^{19}F spin diffusion using crystalline amino acids, where the number of molecules in the asymmetric unit cell is known. We then apply the ^{19}F CODEX technique to protegrin-1 (PG-1), a β-hairpin antimicrobial peptide known to destroy the cell membranes of a variety of microbial organisms.[29,30] Our previous solid-state

(13) Yamaguchi, S.; Hong, T.; Waring, A.; Lehrer, R. I.; Hong, M. *Biochemistry* **2002**, *41*, 9852−9862. Buffy, J. J.; Hong, T.; Waring, A. J.; Lehrer, R. I.; Hong, M. *Biophys. J.* **2003**, *85*, 2363−2373.
(14) Antzutkin, O. N.; Balbach, J. J.; Leapman, R. D.; Rizzo, N. W.; Reed, J.; Tycko, R. *Proc. Natl. Acad. Sci. U.S.A.* **2000**, *97*, 13045−13050.
(15) Antzutkin, O. N.; Tycko, R. *J. Chem. Phys.* **1999**, *110*, 2749−2752.
(16) deAzevedo, E. R.; Bonagamba, T. J.; Hu, W.; Schmidt-Rohr, K. *J. Am. Chem. Soc.* **1999**, *121*, 8411−8412.
(17) Schmidt-Rohr, K.; deAzevedo, E. R.; Bonagamba, T. J. In *Encyclopedia of NMR*; Grant, D. M., Harris, R. K., Eds.; John Wiley & Sons: Chichester, U.K., 2002.
(18) Suter, D.; Ernst, R. R. *Phys. Rev. B* **1985**, *32*, 5608−5627.
(19) Meier, B. H. *Adv. Magn. Opt. Reson.* **1994**, *18*, 1−115.
(20) Tekley, P.; Gardiennet, C.; Potrzebowski, M. J.; Sebald, A.; Reichert, D.; Luz, Z. *J. Chem. Phys.* **2002**, *116*, 7607−7616.
(21) Reichert, D.; Bonagamba, T. J.; Schmidt-Rohr, K. *J. Magn. Reson.* **2001**, *151*, 129−135.
(22) Gilchrist, M. L., Jr.; Monde, K.; Tomita, Y.; Iwashita, T.; Nakanishi, K.; McDermott, A. E. *J. Magn. Reson.* **2001**, *152*, 1−6.
(23) Salgado, J.; Grage, S. L.; Kondejewski, L. H.; Hodges, R. S.; McElhaney, R. N.; Ulrich, A. S. *J. Biomol. NMR* **2001**, *21*, 191−208.
(24) Afonin, S.; Glaser, R. W.; Berditchevskaia, M.; Wadhwani, P.; Guhrs, K. H.; Mollmann, U.; Perner, A.; Ulrich, A. S. *ChemBioChem* **2003**, *4*, 1151−1163.
(25) Glaser, R. W.; Sachse, C.; Durr, U. H.; Wadhwani, P.; Ulrich, A. S. *J. Magn. Reson.* **2004**, *168*, 153−163.
(26) Toke, O.; O'Connor, R. D.; Weldeghiorghis, T. K.; Maloy, W. L.; Glaser, R. W.; Ulrich, A. S.; Schaefer, J. *Biophys. J.* **2004**, *87*, 675−687.
(27) Goetz, J. M.; Poliks, B.; Studelska, D. R.; Fischer, M.; Kugelbrey, K.; Bacher, A.; Cushman, M.; Schaefer, J. *J. Am. Chem. Soc.* **1999**, *121*, 7500−7508.
(28) Wi, S.; Sinha, N.; Hong, M. *J. Am. Chem. Soc.* **2004**, *126*, 12754−12755.
(29) Kokryakov, V. N.; Harwig, S. S.; Panyutich, E. A.; Shevchenko, A. A.; Aleshina, G. M.; Shamova, O. V.; Korneva, H. A.; Lehrer, R. I. *FEBS Lett.* **1993**, *327*, 231−236.

NMR studies showed that the PG-1 backbone is completely immobilized in POPC membranes while rotating uniaxially in thinner DLPC bilayers.[31] The lack of motion in the POPC membrane suggests aggregation in the membrane. The present ^{19}F CODEX experiments, conducted at 223 K when spin diffusion dominates the exchange process, indicate that PG-1 exists predominantly as dimers at a peptide concentration of 7.4%. Lowering the peptide concentration reduced the magnetization exchange, indicating decreased dimer formation. The concentration-dependent dimer fraction yields a free energy change of -10.2 ± 2.3 kJ/mol for the monomer−dimer equilibrium. This is the first time membrane peptide oligomerization has been directly determined structurally in the lipid bilayer.

Materials and Methods

Crystalline L-Phe samples with 4-^{19}F and ^{13}C′ labels were recrystallized from concentrated HCl solutions. The amino acid structure was confirmed using single-crystal X-ray diffraction and found to be identical to the reported structure.[32,33] Crystalline ^{13}C′-labeled Gly contained two polymorphs with distinct isotropic shifts: the major form is α-Gly, and the minor form is γ-Gly. Fluorinated PG-1 (NH_2-RGGRLCYCRRR*F*CVCVGR-$CONH_2$) was synthesized on the 0.25 mmol scale using Fmoc solid-phase peptide synthesis protocols as described before.[13] [^{19}F]-4-fluoro-L-Phe was incorporated at Phe_{12}. [^{13}C′]Val_{16} and [^{15}N]Val_{14} were also incorporated in one sample to confirm the backbone rigidity of the peptide in POPC bilayers at room temperature. Herzfeld−Berger analysis of the CSA sidebands yielded the anisotropy parameter (δ) and the asymmetry parameter (η). Synthesized PG-1 contained residual trifluoroacetic acid and the trifluoroacetate (TFA) counterions. These give rise to a ^{19}F signal at −75 ppm, which partially overlaps with the edge of the rigid-limit ^{19}F CSA sidebands of [^{19}F]-4-fluoro-Phe. Thus, we removed residual TFA by repeated (3−4 times) washing and lyophilization of the peptide in 5 mM HCl solution, until negligible TFA signal was detected in the NMR spectrum. The purified fluorinated peptide was combined with POPC lipids (main phase transition temperature −2 °C) by codissolving them in methanol and chloroform solutions to achieve the desired P:L mole ratio. The combined solution was dried under a stream of nitrogen gas and the resulting membrane film redissolved in a small amount of cyclohexane and lyophilized. The samples were loaded into a 4 mm ZrO_2 rotor equipped with borosilicate glass spacers and directly hydrated to 35% water by mass. ^{31}P spectra of the lipid confirm that the resulting membrane mixture is in the fully hydrated L_α phase at ambient temperature.

NMR experiments were carried out on a Bruker DSX-400 spectrometer (Karlsruhe, Germany) operating at a resonance frequency of 400.49 MHz for ^{1}H, 376.84 MHz for ^{19}F, and 100.70 MHz for ^{13}C. ^{19}F experiments were conducted on an MAS probe with a 4 mm spinner module. A Bruker HFX unit containing a tuning splitter and a power combiner splits the ^{1}H channel of the probe into two channels for simultaneous ^{1}H and ^{19}F radio frequency irradiation. Samples were spun at low temperature using air cooled through a Kinetics Thermal Systems XR air-jet sample cooler (Stone Ridge, NY). The temperature was maintained within ±1 K of the desired value, and the spinning speed was regulated to ±3 Hz. Typical 90° pulse lengths were 5 μs for ^{19}F and ^{13}C and 3.5−4.0 μs for ^{1}H. A short ^{1}H−^{19}F cross-polarization (CP) contact time of 0.3 ms was used, while ^{1}H−^{13}C contact times were 0.5 ms. The typical recycle delays were 2 s, and acquisition times were ~30 ms for ^{13}C and ~3 ms for ^{19}F. ^{13}C and ^{19}F chemical shifts were referenced externally to the α-Gly ^{13}C′ signal at 176.4 ppm on the TMS scale and the Teflon ^{19}F signal at −122 ppm, respectively.

The pulse sequence for the ^{19}F and ^{13}C CODEX experiments is shown in Figure 1a.[16] After CP from ^{1}H, the X spin magnetization evolves under the CSA interaction, which is recoupled by 180° pulses that are spaced at half a rotor period apart.[34] The pair of 90° pulses immediately after CP allows the input of a trigger signal for active rotor synchronization of the two CSA recoupling pulse trains. The total CSA recoupling time, τ_{CSA}, must be sufficiently long to detect small-angle orientational changes. For uniaxial chemical shift tensors, τ_{CSA} needs to satisfy the condition $\delta\tau_{CSA} \sin \beta_R \geq 2$, where β_R is the orientation change.[17] Between the two CSA periods, the magnetization is stored along the z axis for a mixing time, τ_m, without ^{1}H decoupling, during which magnetization undergoes ^{1}H-driven spin diffusion. This changes the CSA frequency, thus reducing the intensity of the stimulated echo. Spin diffusion among M differently oriented sites reduces the echo to a final intensity of $1/M$. To correct for spin−lattice relaxation (T_1) effects during τ_m, a z filter (τ_z) is added at the end of the second π-pulse train. Two experiments were conducted: a dephasing experiment (S) with the desired τ_m and a short z filter (<1 ms) and a reference experiment (S_0) with interchanged τ_m and τ_z values. Due to the short duration of the mixing between the two π-pulse trains, the S_0 experiment does not have spin diffusion but has a total z magnetization time identical to that of the S experiment. Thus, the intensity ratio S/S_0 represents the normalized exchange free of T_1 relaxation. Due to the strong coupling of the X spins to the surrounding protons, the empirically observed normalized exchange signal usually dephases exponentially with τ_m, $S/S_0 = 1/M + \sum_i e^{-\tau_m/\tau_{sd,i}}$, where $\tau_{sd,i}$ is the spin diffusion time constant. A multiexponential decay suggests the presence of multiple and significantly different X−X distances. However, the values of the decay constants cannot be quantitatively related to individual distances.

Results and Discussion

Crystalline Amino Acids. We demonstrate the principle of CODEX spin diffusion for determining the number of unique molecular orientations on two crystalline amino acids, Gly and Phe. α-Gly[35] has four molecules per unit cell, two of which have unique orientations, while γ-Gly[36] contains three magnetically inequivalent molecules per unit cell. ^{13}C CODEX experiments on Gly were conducted using a $\delta\tau_{CSA}$ of 7.2, which is sufficiently large to detect orientational differences as small as ~15°. Figure 2A shows the ^{13}C S/S_0 values as a function of τ_m for both polymorphs of Gly. The CODEX curve decays to an equilibrium value of 0.49 for α-Gly and 0.32 for γ-Gly, consistent with the M values of 2 and 3, respectively. Both curves are well fit by single-exponential decays, with a decay constant of 270 ms for α-Gly and 120 ms for γ-Gly. The distances probed on this time scale are 4−5 Å: the nearest-neighbor C′−C′ distances between unique orientations are 4.22 Å in α-Gly and 4.17 and 5.23 Å in γ-Gly.

The distance reaches of ^{13}C and ^{19}F spin diffusion in the CODEX experiment are compared using crystalline Phe, which has four different molecules per asymmetric unit cell. The *p*-^{19}F site has a chemical shift anisotropy δ of 58 ppm and an asymmetry parameter η of 0.67. The ^{19}F CODEX experiment was conducted at a spinning speed of 9 kHz and with four rotor periods of CSA recoupling. This corresponds to $\delta\tau_{CSA} = 9.7$, which is sufficiently large to detect ~10° orientational differences. The ^{19}F data shown here were acquired at 253 K to

(30) Bellm, L.; Lehrer, R. I.; Ganz, T. *Exp. Opin. Invest. Drugs* **2000**, *9*, 1731−1742.
(31) Buffy, J. J.; Waring, A. J.; Lehrer, R. I.; Hong, M. *Biochemistry* **2003**, *42*, 13725−13734.
(32) Gurskaya, G. V. *Kristallografiya* **1964**, *9*, 839−845.
(33) Al-Karaghouli, A. R.; Koetzle, T. F. *Acta Crystallogr., Sect. B: Struct. Crystallogr. Cryst. Chem.* **1975**, *B31*, 2461−2465.
(34) Gullion, T.; Schaefer, J. *J. Magn. Reson.* **1989**, *81*, 196−200.
(35) Kozhin, V. M. *Kristallografiya* **1978**, *23*, 1211−1215.
(36) Iitaka, Y. *Mineral. J. (Sapporo)* **1958**, *2*, 283−297.

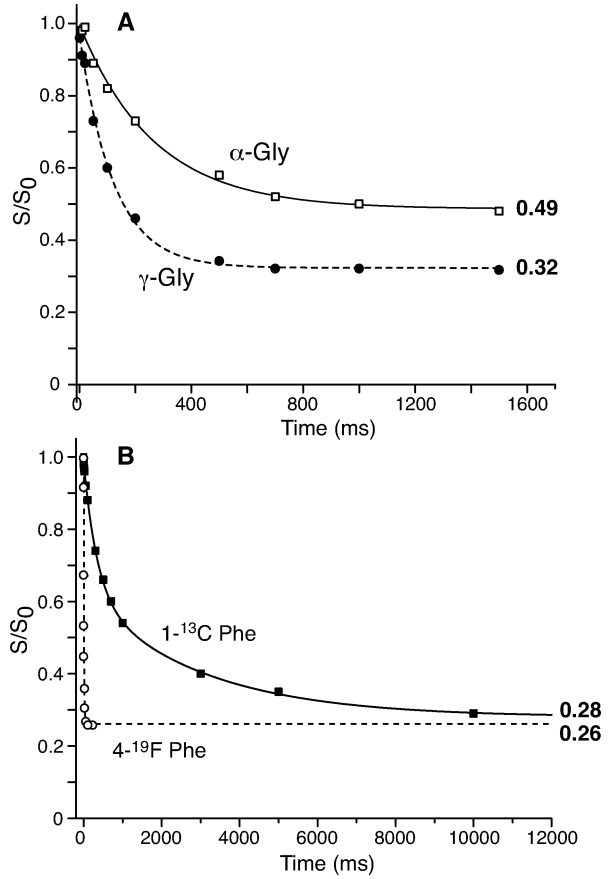

Figure 2. CODEX dephasing curves S/S_0 as a function of mixing time for (A) α-Gly (squares) and γ-Gly (circles) labeled at 1-^{13}C and (B) [1-^{13}C]Phe (squares) and [^{19}F]-4-fluoro-Phe (circles). Single-exponential functions with a constant offset best fit the Gly data in (A), while double-exponential functions best fit the Phe data in (B). The equilibrium value of each dephasing curve agrees with the known number of magnetically inequivalent molecules in each unit cell. Note the 2 orders of magnitude decrease in the spin diffusion equilibration time for ^{19}F CODEX compared to ^{13}C CODEX in (B) due to the stronger ^{19}F−^{19}F dipolar coupling.

eliminate possible side chain motion. However, the CODEX results are identical between 253 and 292 K, indicating that only spin diffusion and no slow motion is present during the mixing time. The ^{13}C′-detected CODEX experiment used $\delta\tau_{CSA} = 3.6$, sufficient for detecting a β_R of ∼30°. Figure 2B shows that the ^{13}C and ^{19}F CODEX curves decay to 0.28 and 0.26, respectively, both consistent with $M = 4$. However, the ^{13}C decay rate is strikingly slower than the ^{19}F decay rate. Both curves are best fit to double exponentials. The ^{13}C decay constants are 350 ms and 3.0 s, while the ^{19}F decay constants are 0.53 and 13 ms, more than 2 orders of magnitude shorter. This time scale difference results mainly from the 14-fold stronger ^{19}F−^{19}F dipolar coupling constant, since the crystal structure of Phe shows the ^{13}C′−^{13}C′ distances to be comparable to the ^{19}F−^{19}F distances, between 3.6 and 14 Å. Moreover, both ^{13}C′−^{13}C′ and ^{19}F−^{19}F distances cluster into two distinct ranges: one short (3.6−5.5 Å) and the other long (11−15 Å), justifying the double-exponential fit.

Thus, the use of ^{19}F spin diffusion over ^{13}C spin diffusion allows the efficient detection of the number of differently oriented molecules within a distance of ∼15 Å. The high γ of the ^{19}F spin and the resulting stronger homonuclear dipolar coupling reduce the time needed to reach complete exchange by 2 orders of magnitude. This is crucial for studying membrane peptides, whose intermolecular distances almost certainly surpass those between small molecules, and whose T_1 relaxation times will be generally shorter than those of crystalline compounds and thus limit the use of long mixing times required for ^{13}C CODEX. The amino acid results indicate that the CODEX time constants qualitatively reflect the internuclear distances. The ^{13}C spin diffusion decay rates of α- and γ-Gly and the fast decay component of [^{13}C′]Phe all have the same order of magnitude (120−350 ms), and correspond to distances of 3.6−5.2 Å. In contrast, ^{13}C−^{13}C distances above 10 Å require more than 1 s to detect.

Lipid-Free [^{19}F]-4-fluoro-PG-1. While ^{19}F CODEX can unequivocally determine orientational inequivalences in amino acids, its ability to measure the number of molecules in peptide aggregates, where the internuclear distances are expected to be much larger, is still untested. Thus, we conducted ^{19}F CODEX experiments on lyophilized [^{19}F]-4-fluoro-PG-1 prior to membrane binding. In the absence of water or lipids, the peptide should be closely packed and have no particular structural order. The intermolecular F−F distances represent a lower limit that the CODEX technique must be able to detect to be useful for membrane-diluted peptides. Figure 3A shows a representative pair of ^{19}F CODEX spectra, for a mixing time of 300 ms, where a significant difference intensity, $\Delta S = S_0 - S$, is observed. The S/S_0 value decays to 0.26 after 1 s, and is best fit to a single-exponential function with $\tau_{sd} = 200$ ms. This demonstrates that ^{19}F spin diffusion is able to detect at least four PG-1 molecules sufficiently aggregated. The decay constant is 1−2 orders of magnitude larger than those of Phe, suggesting that the minimum F−F distance between PG-1 molecules is indeed much longer than in crystalline Phe. The decay of the S_0 signal indicates a ^{19}F T_1 relaxation time of 1.7 s, which is sufficiently long for measuring spin diffusion at long mixing times.

[^{19}F]-4-fluoro-PG-1 in POPC Membranes. To determine whether PG-1 is aggregated in the lipid bilayer, we prepared PG-1/POPC liposomes with a P:L molar ratio of 1:12.5, corresponding to a peptide concentration of 7.4 mol %. This was chosen to exceed the membrane disruption and aggregation thresholds based on our previous NMR experiments. ^{31}P spectra of oriented membranes showed that PG-1 disrupts the POPC membrane order above a concentration of 3.3%,[13] while ^{13}C MAS experiments indicated that the peptide backbone is immobilized in POPC bilayers at a concentration of 4%.[31] Since lipid molecules are dynamic solvents that can induce significant peptide motion, we conducted the ^{19}F CODEX experiments at 223 K. The ^{19}F CSA sideband pattern (not shown) at this temperature gives a δ of 57 ppm and an η of 0.69, comparable to the rigid-limit values measured for lipid-free PG-1. The experiment was conducted at a spinning speed of 8 kHz with two rotor periods of CSA recoupling; thus, $\delta\tau_{CSA} = 5$. Figure 3B shows that the peptide ^{19}F signal decays to a final value of 0.56 ± 0.06 in 1 s with a single-exponential time constant of 225 ms. This equilibrium value indicates that PG-1 mainly associates as dimers in POPC membranes. The fact that the equilibrium value is slightly higher than 0.50 suggests that a small fraction of the peptide remains as monomers. Then the measured S/S_0 is the weighted average of the values of the monomer ($S/S_0 = 1$) and dimer ($S/S_0 = 0.5$). The fraction of the dimer, f_D, can be obtained from $0.5f_D + 1(1 - f_D) = 0.56$, resulting in $f_D = 88\%$. The single-exponential fit indicates that

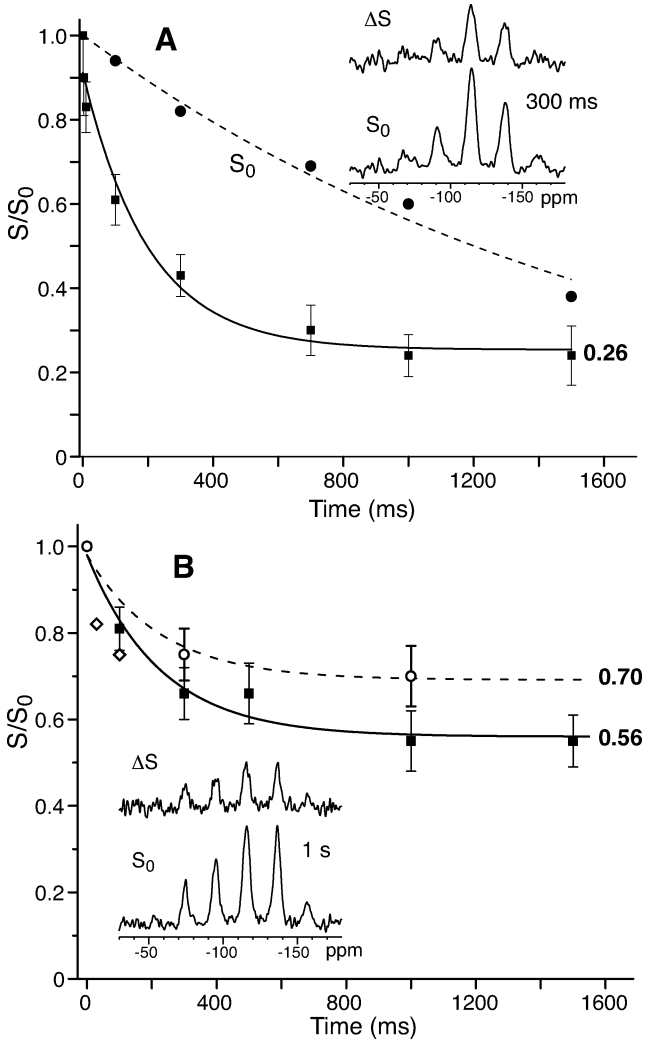

Figure 3. CODEX dephasing curves S/S_0 for PG-1. (A) Lipid-free PG-1. A representative set of S_0 and ΔS spectra are shown. S/S_0 decays to ~0.25, indicating at least four PG-1 molecules are aggregated in close proximity. The ^{19}F T_1, measured from the S_0 decay, is 1.7 s. (B) PG-1 bound to POPC lipids at 223 K. A representative set of S_0 and ΔS spectra are shown. Key: filled squares and solid line, 7.4% PG-1 concentration; open circles, 2.8% PG-1; open tilted squares between 0 and 200 ms, CODEX with ^{1}H decoupling during the mixing time for the 7.4% PG-1/POPC sample. The reduction of the S/S_0 values with ^{1}H decoupling indicates spin diffusion to be the main exchange mechanism.

there is only a single resolvable ^{19}F−^{19}F intermolecular distance, in contrast to the amino acid Phe. This suggests that there are no higher order aggregates such as tetramers coexisting with monomers and dimers, since this would entail multiple intermolecular F−F distances.

It is important to verify that the observed exchange at 223 K is due to spin diffusion rather than slow peptide motion. Two types of motion could occur in the Phe side chain: phenylene ring flip and rotation around the Cα−Cβ bond. The former does not change the *p*-^{19}F position or the F−F dipolar coupling. The latter is unlikely at 223 K on the basis of the similarity of the PG-1 ^{19}F CSA to that of crystalline Phe, which has no χ_1 torsion dynamics on either the fast or slow time scales, as determined by the rigid-limit Cβ−Hβ dipolar coupling[28] and the invariance of its CODEX curve to temperature changes. To verify the lack of slow motion in PG-1 at 223 K, we carried out a CODEX experiment with ^{1}H decoupling active during τ_m. For sites with identical isotropic chemical shifts but different anisotropic shifts, ^{1}H decoupling during τ_m speeds up spin diffusion by increasing the overlap integral $f_{ij}(0)$[37,38] but does not affect motional exchange. Thus, if spin diffusion is the main mechanism of exchange, lower S/S_0 values are expected with ^{1}H decoupling than without. We applied moderate ^{1}H decoupling field strengths of 50 and 30 kHz for 30 and 100 ms, respectively, due to the shared use of the ^{1}H channel for both ^{1}H and ^{19}F irradiation. Figure 3B shows that the two S/S_0 values acquired using ^{1}H decoupling (tilted squares) are indeed lower than the values without ^{1}H decoupling, thus confirming that spin diffusion is the dominant exchange mechanism at this temperature.

Interestingly, at 292 K the Phe side chain of PG-1 exhibits fast motion: the ^{19}F CSA is averaged to $\bar{\delta} = -28$ ppm and $\bar{\eta} = 1.0$. This suggests that the liquid-crystalline bilayer indeed promotes significant side chain conformational motion, a phenomenon that has been observed previously.[39,40] The corresponding CODEX curve (Supporting Information Figure S1) shows a ~25% component of fast decay ($\tau_{sd,1} \approx 10$ ms), which we attribute to χ_1 torsion dynamics on a time scale near the CODEX detection limit. The remaining nonmotional exchange can be fit excellently, although not uniquely, by equal weights (~37%) of a constant offset and a slow decaying component with a $\tau_{sd,2}$ of ~1.5 s. We attribute this to ^{19}F spin diffusion, where the equal weights are consistent with dimer formation of the peptide concluded at low temperature. The fact that the slow diffusion time constant is much larger at 292 K is understandable since the ^{19}F−^{19}F dipolar coupling is attenuated by motion, decreasing the coupling parameter, K_{ij}.

Our previous ^{31}P spectra of oriented POPC membranes containing PG-1 indicate that the bilayer structure is severely disrupted above a peptide concentration of 3.3%.[13] To determine if PG-1 aggregation depends on the concentration and potentially correlates with bilayer disruption, we conducted the CODEX experiment at a lower P:L of 1:34.5, corresponding to a peptide concentration of 2.8%. Due to the lower sensitivity, only two mixing times, 300 ms and 1 s, were measured. Figure 3B shows that the diluted PG-1 sample gives an S/S_0 of 0.75 at 300 ms and 0.70 at 1 s (circles). The latter value is most likely the equilibrium value, since the difference between the two data points is small and the 7.4% sample has equilibrated at 1 s. The error bar indicates that the difference of this S/S_0 value from that of the concentrated sample is statistically significant. The higher equilibrium value indicates an increased fraction of monomers. Since the higher concentration data support monomer−dimer equilibrium, the more dilute sample cannot have higher order aggregates. Thus, the equilibrium value of 0.70 corresponds to a dimer fraction of 60% and a monomer fraction of 40%. Moreover, the best fit for the 2.8% CODEX data has the same decay constant as that for the 7.4% sample within experimental uncertainty. This indicates that the dimers that do form at lower concentration have a structure similar to that of the high-concentration sample.

Aggregation Model of PG-1 in POPC Membranes. Antimicrobial peptides, part of the innate immune system of many

(37) Bronniman, C. E.; Szeverenyi, N. M.; Maciel, G. E. *J. Chem. Phys.* **1983**, *79*, 3694−3700.
(38) Reichert, D.; Hempel, G.; Poupko, R.; Luz, Z.; Olejniczak, Z.; Tekely, P. *Solid State Nucl. Magn. Reson.* **1998**, *13*, 137−148.
(39) Mueller, L.; Frey, M. H.; Rockwell, A. L.; Gierasch, L. M.; Opella, S. J. *Biochemistry* **1986**, *25*, 557−561.
(40) Opella, S. J. *Methods Enzymol.* **1986**, *131*, 327−361.

organisms against bacterial, fungal, and viral attacks,[41] are thought to kill invading microbes by destroying their cell membranes via aggregation or oligomerization. Three leading models have emerged for describing the mode of action of these small defensive peptides. The barrel-stave model postulates that transmembrane peptides form helical bundles[42,43] that deplete the membrane potential. The carpet model hypothesizes that peptides aggregate on the surface of the membrane at low concentrations, but at high concentrations they micellize the bilayer, thus destroying the membrane.[44] The toroidal-pore model suggests that aggregated peptides form pores where the lipid orientations change, connecting the upper and lower leaflets of the bilayer.[45] Although oligomerization is central to all these models, there is so far little direct evidence of peptide aggregation[46] due to the lack of suitable techniques. The spin diffusion NMR technique presented here is thus relevant for determining the aggregation of these membrane-active peptides in the lipid membrane.

Evidence of PG-1 aggregation in DPC micelles was reported based on ^{1}H NOEs between residues far apart in the β-hairpin structure, and based on the slowness of ^{1}H/^{2}H exchange for amide hydrogens not involved in intramolecular hydrogen bonds.[47] These data indicated an antiparallel dimer, with the C-terminal strands adjacent to each other, in an NCCN fashion. Although further association of the dimer was hypothesized, evidence for it was lacking, since no intermolecular NOEs for such higher order aggregates were observed.[47] The current ^{19}F CODEX data indicate that, in the lipid bilayer at a peptide concentration of 7.4%, PG-1 mainly (88%) exists as dimers. Although the CODEX experiment presented here in principle cannot simultaneously determine both the fraction and the size of the aggregate in a heterogeneous mixture, the scenario of having higher order oligomers rather than dimers in PG-1 is unlikely for several reasons. First, the CODEX decay curve is single exponential (Figure 3B); thus, only a single oligomeric species (other than a monomer) is present, and a complex equilibrium such as monomer−dimer−tetramer can be ruled out. Second, if the sample consisted of monomers and tetramers, then the fraction of the monomer would be very high, 40%, to give the observed equilibrium value of 0.56. For such different molecular weight species to both be present at significant percentages, there should be observable chemical shift and line width distribution in the ^{13}C, ^{15}N, and ^{19}F spectra of the peptide. No such spectral heterogeneity was observed (Supporting Information Figure S2). Finally, other membrane peptides whose oligomerization has been characterized are completely oligomerized at concentrations above 1%.[6]

Modeling of the PG-1 structure (PDB accession code 1PG1)[48] suggests that the ^{19}F−^{19}F distances in both parallel and antiparallel NCCN dimers are 11−14 Å, a distance range that is accessible by ^{19}F CODEX (Figure 4A). More detailed distance measurements are required to further delineate the structure of the dimer interface.

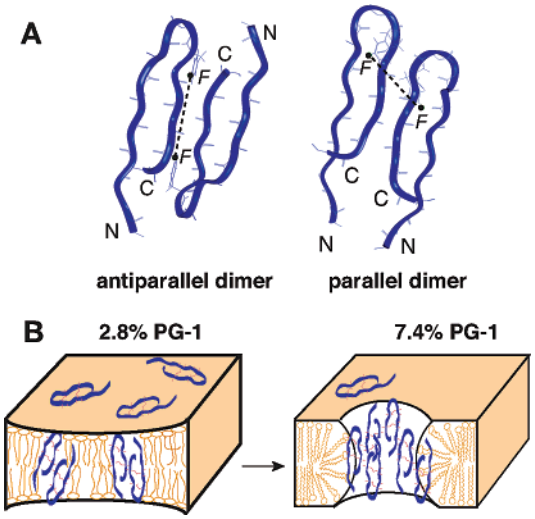

Figure 4. Model of PG-1 dimerization in POPC membranes. (A) Antiparallel and parallel NCCN dimers of PG-1. The solution NMR PG-1 structure is used. The dimers are modeled to satisfy intermolecular hydrogen bonds between the two C-terminal strands. The F−F distances in the model are 11−14 Å, which are measurable by the spin diffusion technique. (B) Concentration dependence of PG-1 dimerization. At a concentration of 2.8%, 60% of the peptide is dimerized, and the membrane is only slightly distorted. The monomeric peptide likely remains on the membrane surface. At a peptide concentration of 7.4%, the dimer fraction increases to ~90% and creates significant membrane disorder.

A PG-1 dimer appears too small to be completely immobilized in the POPC membrane at room temperature.[13,31] On the basis of the size and viscosity dependence of rotational diffusion rates in two-dimensional lipid membranes,[49] one would expect the PG-1 dimer to undergo whole-body uniaxial rotation. We hypothesize that the reason for the lack of this overall mobility is the hydrophobic mismatch between the lipid bilayer and the PG-1 dimer. This hydrophobic mismatch may induce highly curved membrane defects that trap the PG-1 dimers (Figure 4B, right). Evidence of such membrane defects is seen from the distorted ^{31}P line shape of the POPC membrane in the presence of PG-1[13] and the emergence of an isotropic ^{31}P peak when anionic POPG lipids are added to the membrane.[50] In addition, it is possible that loose aggregates of dimers may exist to line the defects in the lipid membrane. Such larger aggregates of dimers may not be detectable on the ^{19}F spin diffusion length scale.

Figure 4B summarizes our current model of PG-1 dimerization and its relation to its membrane disruptive function. We postulate that dimerization is required to maximize peptide insertion into the membrane. The oligomeric peptides create structural defects in the membrane, as manifested in the ^{31}P NMR line shape.[13] These defects in turn constrain the peptide and prevent it from undergoing whole-body rotation. At low concentrations, more peptides are monomeric and may remain on the membrane surface, as indicated by X-ray lamellar diffraction and oriented circular dichroism data.[51,52]

(41) Hancock, R. E.; Lehrer, R. *Trends Biotechnol.* **1998**, *16*, 82−88.
(42) He, K.; Ludtke, S. J.; Worcester, D. L.; Huang, H. W. *Biophys. J.* **1996**, *70*, 2659−2666.
(43) Duclohier, H.; Wroblewski, H. *J. Membr. Biol.* **2001**, *184*, 1−12.
(44) Pouny, Y.; Rapaport, D.; Mor, A.; Nicolas, P.; Shai, Y. *Biochemistry* **1992**, *31*, 12416−12423.
(45) Matsuzaki, K. *Biochim. Biophys. Acta* **1998**, *1376*, 391−400.
(46) Epand, R. M.; Vogel, H. J. *Biochim. Biophys. Acta* **1999**, *1462*, 11−28.
(47) Roumestand, C.; Louis, V.; Aumelas, A.; Grassy, G.; Calas, B.; Chavanieu, A. *FEBS Lett.* **1998**, *421*, 263−267.
(48) Fahrner, R. L.; Dieckmann, T.; Harwig, S. S.; Lehrer, R. I.; Eisenberg, D.; Feigon, J. *Chem. Biol.* **1996**, *3*, 543−550.
(49) Saffman, P. G.; Delbruck, M. *Proc. Natl. Acad. Sci. U.S.A.* **1975**, *72*, 3111−3113.
(50) Mani, R.; Buffy, J. J.; Waring, A. J.; Lehrer, R. I.; Hong, M. *Biochemistry*, in press.
(51) Heller, W. T.; Waring, A. J.; Lehrer, R. I.; Huang, H. W. *Biochemistry* **1998**, *37*, 17331−17338.
(52) Heller, W. T.; Waring, A. J.; Lehrer, R. I.; Harroun, T. A.; Weiss, T. M.; Yang, L.; Huang, H. W. *Biochemistry* **2000**, *39*, 139−145.

Energetics of PG-1 Dimer Formation in POPC Membranes. We can estimate the free energy of PG-1 dimer formation, ΔG, using a simple monomer (M)−dimer (D) equilibrium model, $2M \rightleftharpoons D$. The equilibrium association constant, K_a, is $[D]/[M]^2$, where [D] and [M] depend on the peptide concentration, c, and dimer fraction f_D as $[D] = cf_D/2$ and $[M] = c(1 - f_D)$. ΔG is determined from K_a according to $\Delta G = -RT \ln K_a$. On the basis of the experimental data, we found a ΔG of -10.2 ± 2.3 kJ/mol in favor of dimer formation.

What is the driving force for PG-1 dimerization? We postulate that it is primarily the formation of intermolecular hydrogen bonds, which reduces polar interactions in the membrane. Reduced exposure of polar side chains to the membrane[9] may also contribute. On the basis of equilibrium dialysis experiments on model peptides transferred from aqueous solution to membrane environments,[8] White and co-workers estimated the free energy reduction for β-sheet aggregation in the membrane to be ~0.5 kcal/mol (2.09 kJ/mol) per residue,[53] which is also the value per hydrogen bond. Since three residues on the C-terminus strand of PG-1 can form intermolecular hydrogen bonds, a total of six intermolecular hydrogen bonds may be gained per molecule due to aggregation. Thus, the total free energy reduction is ~12.6 kJ/mol, in good agreement with the NMR-deduced energy change.

The free energy estimation further argues against a monomer−tetramer equilibrium for PG-1, since the equilibrium mole fractions in that model would correspond to a small free energy change of −5.6 kJ/mol, which is inconsistent with the number of intermolecular hydrogen bonds that would be formed in a tetramer.

Conclusion

We have shown the utility of ^{19}F CODEX for determining the aggregation of peptides bound to lipid membranes. Demonstration on crystalline amino acids proves unambiguously that the equilibrium exchange value, S/S_0, is indicative of the number of unique orientations in the unit cell. The use of the ^{19}F spin instead of ^{13}C significantly reduces the time required to reach complete exchange, thus increasing the distance reach of ^{1}H-driven spin diffusion. Application of the ^{19}F CODEX technique to the membrane-bound antimicrobial peptide PG-1 at low temperature where peptide motions are frozen indicates that, at a concentration of 7.4%, PG-1 exists predominantly as dimers in POPC membranes. This is consistent with the observation of PG-1 in DPC micelles in solution. Lowering the peptide concentration reduced the dimer fraction. On the basis of the equilibrium constant, we estimate the free energy reduction for dimer formation to be ~10.2 kJ/mol. This is in good agreement with the previously measured free energy change of β-sheet aggregation, and supports the view that the main driving force for PG-1 aggregation is the formation of intermolecular hydrogen bonds.

We anticipate this ^{19}F spin diffusion approach to be generally applicable to the study of the association of peptides in complex environments, such as membrane peptides that form channels in lipid membranes,[54,55] coiled coil proteins, and amyloid peptides. For peptides that exist in more complex equilibria with multiple oligomerization states, the basic CODEX pulse sequence may be concatenated into a four-time CODEX experiment[56] to detect the spin diffusion of only those molecules that are part of an aggregate. By removing the monomer signals and selectively detecting the aggregate signals, one may be able to obtain additional constraints to determine both the fractions and the sizes of the aggregates in such mixtures.

Acknowledgment. This work is supported by NIH Grants GM-066976 to M.H. and AI-22839 and AI-37945 to A.J.W. and R. I. Lehrer. We thank R. Mani for help in the Phe experiments.

Supporting Information Available: ^{19}F CODEX data of PG-1 at room temperature and ^{13}C and ^{15}N MAS spectra of the 7.4% PG-1 sample (PDF). This material is available free of charge via the Internet at http://pubs.acs.org.

JA043621R

(53) White, S. H.; Wimley, W. C. *Annu. Rev. Biophys. Biomol. Struct.* **1999**, *28*, 319−365.
(54) Pinto, L. H.; Dieckmann, G. R.; Gandhi, C. S.; Papworth, C. G.; Braman, J.; Shaughnessy, M. A.; Lear, J. D.; Lamb, R. A.; DeGrado, W. F. *Proc. Natl. Acad. Sci. U.S.A.* **1997**, *94*, 11301−11306.
(55) Nishimura, K.; Kim, S.; Zhang, L.; Cross, T. A. *Biochemistry* **2002**, *41*, 13170−13177.
(56) deAzevedo, E. R.; Bonagamba, T. J.; Hu, W.; Schmidt-Rohr, K. *J. Chem. Phys.* **2000**, *112*, 8988−9001.
(57) Bennett, A. E.; Rienstra, C. M.; Auger, M.; Lakshmi, K. V.; Griffin, R. G. *J. Chem. Phys.* **1995**, *103*, 6951−6958.